Original Article

JCBFM

Journal of Cerebral Blood Flow & Metabolism
2020, Vol. 40(1) 150–162

DOI: 10.1177/0271678X18806640
journals.sagepub.com/home/jcbfm
SAGE

Age dependency of cerebral P-glycoprotein function in wild-type and APPPS1 mice measured with PET

Viktoria Zoufal[1], Thomas Wanek[1], Markus Krohn[2], Severin Mairinger[1], Thomas Filip[1], Michael Sauberer[1], Johann Stanek[1], Thomas Pekar[3], Martin Bauer[4], Jens Pahnke[2,5,6,7] and Oliver Langer[1,4,8]

Abstract

P-glycoprotein (P-gp, ABCB1) is an efflux transporter at the blood–brain barrier (BBB), which mediates clearance of beta-amyloid (Aβ) from brain into blood. We used (*R*)-[^{11}C]verapamil PET in combination with partial P-gp inhibition with tariquidar to measure cerebral P-gp function in a beta-amyloidosis mouse model (APPtg) and in control mice at three different ages (50, 200 and 380 days). Following tariquidar pre-treatment (4 mg/kg), whole brain-to-plasma radioactivity concentration ratios ($K_{p,brain}$) were significantly higher in APPtg than in wild-type mice aged 50 days, pointing to decreased cerebral P-gp function. Moreover, we found an age-dependent decrease in cerebral P-gp function in both wild-type and APPtg mice of up to −50%. Alterations in P-gp function were more pronounced in Aβ-rich brain regions (hippocampus, cortex) than in a control region with negligible Aβ load (cerebellum). PET results were confirmed by immunohistochemical staining of P-gp in brain microvessels. Our results confirm previous findings of reduced P-gp function in Alzheimer's disease mouse models and show that our PET protocol possesses adequate sensitivity to measure these functional changes in vivo. Our PET protocol may find use in clinical studies to test the efficacy of drugs to induce P-gp function at the human BBB to enhance Aβ clearance.

Keywords

Alzheimer's disease, APPPS1 mice, beta-amyloid, blood–brain barrier, P-glycoprotein

Received 25 June 2018; Revised 3 September 2018; Accepted 9 September 2018

Introduction

Major pathohistological hallmarks of Alzheimer's disease (AD) are the accumulation of beta-amyloid (Aβ) plaques and neurofibrillary tangles consisting of hyperphosphorylated tau protein in the brain.[1] The amyloid hypothesis suggests that the accumulation of Aβ peptides is the central event triggering neuronal degeneration.[2] It has been suggested that reduced Aβ clearance, rather than increased Aβ production, underlies to a large extent Aβ brain accumulation.[3,4] Aβ clearance from brain to blood occurs via two steps. Aβ first has to pass through the abluminal (brain-facing) and then the luminal (blood-facing) plasma membranes of brain capillary endothelial cells comprising the blood–brain barrier (BBB). Both steps appear to be facilitated, involving transporters or receptors. At the abluminal

[1]Center for Health & Bioresources, AIT Austrian Institute of Technology GmbH, Seibersdorf, Austria
[2]Department of Neuro/Pathology, University of Oslo (UiO) and Oslo University Hospital (OUS), Oslo, Norway
[3]University of Applied Sciences, Wiener Neustadt, Austria
[4]Department of Clinical Pharmacology, Medical University of Vienna, Vienna, Austria
[5]LIED, University of Lübeck, Lübeck, Germany
[6]Leibniz-Institute of Plant Biochemistry, Halle, Germany
[7]Department of Pharmacology, University of Latvia, Rīga, Latvia
[8]Department of Biomedical Imaging und Image-Guided Therapy, Division of Nuclear Medicine, Medical University of Vienna, Vienna, Austria

Corresponding author:
Thomas Wanek, Biomedical Systems, Center for Health & Bioresources, AIT Austrian Institute of Technology GmbH, Seibersdorf 2444, Austria.
Email: thomas.wanek@ait.ac.at

membrane, the low-density lipoprotein receptor-related protein 1 (LRP1) was shown to be responsible for Aβ transfer from brain parenchyma into capillary endothelial cells.[5,6] There is accumulating evidence that Aβ efflux across the luminal endothelial membrane of the BBB into the blood is mediated by the adenosine triphosphate-binding cassette (ABC) transporter P-glycoprotein (P-gp, ABCB1).[3,7–10] Data from AD mouse models[8,11] and from AD patients[12–16] give evidence of an AD pathology-related decrease in cerebral P-gp expression and function. Therefore, numerous attempts have been made in preclinical studies to pharmacologically activate P-gp function at the BBB to enhance Aβ clearance from the brain.[8,17–20] For a future translation of these treatment approaches to humans, methodology is needed to measure P-gp function at the human BBB in vivo.

A useful tool to assess P-gp function in humans is the nuclear imaging technique positron emission tomography (PET) in combination with radiolabeled P-gp substrates, such as racemic [^{11}C]verapamil, (*R*)-[^{11}C]verapamil or [^{11}C]*N*-desmethyl-loperamide.[21,22] These radiotracers have been proven to be suitable for measuring the effect of P-gp inhibition with cyclosporine A or tariquidar on cerebral P-gp function in animals and humans.[23–27] However, these radiotracers possess a limited sensitivity to detect moderate changes in cerebral P-gp expression/function occurring in different neurological diseases, such as AD. This has been attributed to the fact that P-gp is a high-capacity transporter, which can functionally compensate moderate changes in its expression, so that the brain distribution of these radiotracers remains unaltered.[28,29] We have introduced an (*R*)-[^{11}C] verapamil PET imaging protocol with an improved sensitivity, which is based on pre-treatment of subjects with the third-generation P-gp inhibitor tariquidar at a dose, which partially (incompletely) blocks P-gp at the BBB.[25] The principle of this concept is that partial P-gp inhibition decreases the transport capacity of P-gp to an extent that moderate changes in P-gp expression can no longer be functionally compensated, so that they manifest themselves in changes in (*R*)-[^{11}C]verapamil brain distribution. Our PET protocol has already been successfully applied to demonstrate a P-gp up-regulation in a rat epilepsy model[30] and in human epilepsy patients.[31] In addition, it was used to detect a decrease in P-gp function in elderly versus young healthy human volunteers.[32] A similar partial P-gp inhibition protocol has been used in combination with the P-gp substrate radiotracer [^{18}F]MPPF to detect a regional up-regulation of cerebral P-gp in a rat model of pharmacoresistant epilepsy.[33,34]

The aim of this work was to use (*R*)-[^{11}C]verapamil PET in combination with partial P-gp inhibition to measure cerebral P-gp function in a beta-amyloidosis mouse model (APPtg mice)[35] and in wild-type control mice at three different ages (50, 200 and 380 days). To complement our in vivo PET data, animal brains were analyzed immunohistochemically for P-gp levels and for Aβ load.

Materials and methods

Chemicals

Unless otherwise stated, all chemicals were purchased from Sigma-Aldrich (Schnelldorf, Germany) or Merck (Darmstadt, Germany). The P-gp inhibitor tariquidar dimesylate was obtained from Haoyuan Chemexpress Co., Ltd (Shanghai, PRC). Tariquidar dimesylate was freshly dissolved in 2.5% (w/v) aqueous (aq.) dextrose solution before each administration and injected intravenously (i.v.) into mice at a volume of 4 mL/kg body weight.

Animals

Female transgenic mice, which express mutated human amyloid precursor protein (APP) and presenilin 1 (PS1) under control of the Thy1-promoter ($APP_{KM670/671NL}$, PS_{L166P}), with a C57BL6/J genetic background (APPPS1, referred to as APPtg mice)[35] and female wild-type mice with a C57BL/6 J genetic background were used in 3 different age groups of approximately 50 days (mean age: 51 ± 4 days, range: 45–59 days, mean weight: 18.4 ± 1.6 g), 200 days (mean age: 203 ± 6 days, range: 190-213 days, mean weight: 25.4 ± 2.5 g) and 380 days (mean age: 380 ± 4 days, range: 376–388 days, mean weight: 33.9 ± 5.3 g). In addition, a group of female heterozygous Abcb1a/b$^{(+/-)}$ mice with a C57BL/6 J genetic background aged 49 days was used (mean weight: 19.0 ± 2.4 g). In total, 111 mice were used in the experiments. All animals were housed in type III IVC cages under controlled environmental conditions (22 ± 3°C, 40% to 70% humidity, 12-h light/dark cycle) with free access to standard laboratory animal diet (ssniff R/M-H, ssniff Spezialdiäten GmbH, Soest, Germany) and water. An acclimatization period of at least one week was allowed before the animals were used in the experiments. The study was approved by the national authorities (Amt der Niederösterreichischen Landesregierung) and study procedures were in accordance with the European Communities Council Directive of September 22, 2010 (2010/63/EU). The animal experimental data reported in this study are in compliance with ARRIVE (Animal Research: Reporting in Vivo Experiments) guidelines.

Experimental design

An overview of animal groups examined in this study is given in Table 1. Groups of wild-type and APPtg mice aged 50, 200 and 380 days, and heterozygous Abcb1a/b$^{(+/-)}$ mice underwent a PET scan with (*R*)-[^{11}C]verapamil either at 120 min after i.v. injection of vehicle solution (2.5% dextrose) or after injection of tariquidar (4 mg/kg or 15 mg/kg). The dose of tariquidar was selected based on previous work to obtain partial inhibition of P-gp at the BBB.[28]

PET imaging

Imaging experiments were performed under isoflurane anesthesia (2.5–3.5% in air). Animals were warmed throughout the experiment and body temperature and respiratory rate were constantly monitored. Mice were placed in a custom-made imaging chamber and the lateral tail vein was cannulated for i.v. administration. A microPET Focus220 scanner (Siemens Medical Solutions, Knoxville, TN, USA) was used for PET imaging. Mice were i.v. pre-treated under anesthesia either with vehicle solution (2.5% (w/v) aq. dextrose), or with tariquidar (4 mg/kg or 15 mg/kg) at 120 min before start of the PET scan. Dynamic emission scans (60 min) were started with the i.v. injection of (*R*)-[^{11}C]verapamil (37 ± 7 MBq in a volume of 0.1 mL physiological saline solution (0.9%, w/v) containing 0.1% (v/v) polysorbate 80, corresponding to 1.7 ± 0.8 nmol of unlabeled compound). List-mode data were acquired with a timing window of 6 ns and an energy window of 250–750 keV. At the end of the PET scan, a blood sample (20–30 µL) was collected from the retro-orbital venous plexus and animals were sacrificed by cervical dislocation. Blood was centrifuged ($13000 \times g$, 4°C, 4 min) to obtain plasma, and whole brains were removed and embedded in Tissue Freezing Medium (Tissue-Tek O.C.T Compound, Sakura Finetek) for immunohistochemistry. Aliquots of blood and plasma were transferred into pre-weighed tubes and measured for radioactivity in a gamma counter (Wizard 1470, PerkinElmer, Wellesley, MA, USA). The measured radioactivity data were corrected for radioactive decay and expressed as standardized uptake value ((radioactivity per g/injected radioactivity) × body weight). Plasma samples were analyzed with radio-thin-layer chromatography (radio-TLC) for radiolabeled metabolites of (*R*)-[^{11}C]verapamil as described in detail elsewhere.[28]

Table 1. Overview of examined animal groups and numbers.

	Age (days)		
Group	50	200	380
Wild-type vehicle	5	4	5
Wild-type tariquidar (4 mg/kg)	6	5	5
Wild-type tariquidar (15 mg/kg)	5	5	3
APPtg vehicle	5	4	4
APPtg tariquidar (4 mg/kg)	6	6	2[a]
APPtg tariquidar (15 mg/kg)	5	3	–
Abcb1a/b$^{(+/-)}$ vehicle	4	–	–
Abcb1a/b$^{(+/-)}$ tariquidar (4 mg/kg)	4	–	–

[a]Small sample size was caused by animal losses during anesthesia.

PET data analysis

The dynamic PET data were binned into 22 frames, which incrementally increased in time length. PET images were reconstructed using Fourier re-binning of the three-dimensional sinograms followed by a two-dimensional filtered back-projection with a ramp filter giving a voxel size of $0.4 \times 0.4 \times 0.796\,\text{mm}^3$. Using PMOD software (version 3.6, PMOD Technologies Ltd., Zurich, Switzerland), whole brain, cortex, hippocampus and cerebellum were outlined on the PET images using the Mirrione Mouse Atlas and guided by representative magnetic resonance (MR) images obtained in a few animals on a 1 Tesla benchtop MR scanner (ICON, Bruker BioSpin GmbH, Ettlingen Germany). Regions of interest were manually adjusted if necessary to derive time-activity curves (TACs) expressed in SUV units. (*R*)-[^{11}C]verapamil brain uptake was expressed as the brain-to-plasma concentration ratio of radioactivity in the last PET frame ($K_{\text{p,brain}}$). $K_{\text{p,brain}}$ was obtained by dividing the radioactivity concentration measured with PET in the last time frame (from 50 min to 60 min after radiotracer injection) by the radioactivity concentration measured with the gamma counter in the venous plasma sample collected at the end of the PET scan.

Immunohistochemistry

After the PET scan, brains were immediately dissected, incubated in 30% sucrose solution and embedded in Tissue-Tek. Samples were snap frozen in liquid nitrogen and stored at −80°C. After defrosting from −80°C to −20°C, brains were cut in coronal 10 µm thick slices with a cryostat (Microm HM 550, Walldorf, Germany). Frozen sections of three brain regions including cortex, hippocampus and cerebellum were mounted on coated slides (VWR Superfrost Plus) and stored at −80°C. Later, the thawed brain slices were fixed either with 4% paraformaldehyde for P-gp staining or with methanol/acetone (1:1) for Aβ staining. After that, the slides

were unmasked with acetic acid/ethanol (1:3) at −20°C for P-gp immunohistochemistry, washed in 0.1 M tris-buffered saline (TBS) and placed in endogenous peroxidase blocking solution consisting of 0.5% H_2O_2 (v/v) for 30 min. Afterwards, slides were washed and inserted into cover plates (Thermo Scientific™ Shandon™ Glass Coverplates, Fisher Scientific) to achieve standardized staining results. To avoid non-specific reactions, blocking solution was added for 1 h at room temperature. Brain slices were then incubated with the respective primary antibody (1:200, anti-P-glycoprotein antibody (EPR10364), Abcam; 1:300, Anti-beta Amyloid antibody (ab3539), Abcam) or with antibody carrier solution for the negative control at 4°C overnight. The next day, the slides were rinsed with TBS and the secondary antibody (1:500, Biotin-SP (long spacer) AffiniPure Donkey Anti-Rabbit IgG (H+L), Jackson Immuno Research) was applied at room temperature for 60 min. After three washing steps, antibody signals were amplified with the VectaStain ABC-Kit (Vector Laboratories) for 60 min at room temperature. After rinsing the slides with TBS, slides were incubated in nickel/diaminobenzidine solution for visualization of P-gp or Aβ. Slides were washed, dehydrated and mounted with Entellan®. For the semi-quantitative evaluation of stained microvessels or Aβ plaques in the hippocampus, cortex or cerebellum four visual fields (20 × magnification) per mouse ($n = 3$–5 animals per group) were counted and the mean of each group was calculated.

Statistical analysis

Differences between two groups were analyzed by a two-sided *t*-test and between multiple groups by one-way ANOVA followed by a Tukey's multiple comparison test using Prism 7 software (GraphPad Software, La Jolla, CA, USA). To assess correlations, the Pearson correlation coefficient *r* was calculated. The level of statistical significance was set to a *P* value of less than 0.05. All values are given as mean ± standard deviation (SD).

Results

We used (*R*)-[^{11}C]verapamil PET in combination with partial P-gp inhibition with tariquidar to measure cerebral P-gp function in groups of wild-type and APPtg mice aged 50, 200 and 380 days, respectively. We examined heterozygous P-gp knockout mice (Abcb1a/b$^{(+/-)}$) as a control group with a 50% reduction in P-gp expression. In Table 1, an overview of all examined animal groups and corresponding animal numbers is given. To prove that a tariquidar dose of 4 mg/kg resulted in partial P-gp inhibition, we also performed (*R*)-[^{11}C]verapamil PET scans after administration of 15 mg/kg tariquidar in all groups of animals except the 380 days-old APPtg group and the Abcb1a/b$^{(+/-)}$ group (Supplementary Figure 1). As an outcome parameter of (*R*)-[^{11}C]verapamil brain distribution, we determined the brain-to-plasma radioactivity concentration ratio at the end of the PET scan ($K_{p,brain}$). In all groups, whole brain $K_{p,brain}$ values were significantly higher in animals pre-treated with the 15 mg/kg than with the 4 mg/kg tariquidar dose, which supported that the 4 mg/kg tariquidar dose led to partial P-gp inhibition (Supplementary Figure 1). In Figure 1, PET summation images are shown for all groups pre-treated either with vehicle or with 4 mg/kg tariquidar. In Supplementary Figure 2, the corresponding whole brain TACs are shown. While whole brain TACs of all vehicle-pre-treated groups were almost superimposable (Supplementary Figure 2(a)), the TACs diverged from each other in the tariquidar pre-treated groups (Supplementary Figure 2(b)). Accordingly, whole brain $K_{p,brain}$ values were not significantly different among different vehicle-treated groups (Figure 2(a), Supplementary Table 1), while significant differences were found between the tariquidar pre-treated groups (Figure 2(b), Supplementary Table 1). In tariquidar pre-treated wild-type animals, whole brain $K_{p,brain}$ values were significantly higher (indicating decreased P-gp function) in the 200 and 380 than in the 50 days-old group, respectively. In tariquidar pre-treated APPtg animals, there was a clear trend for higher whole brain $K_{p,brain}$ values in the 380 than in the 50 days-old group, but a statistical comparison was hampered by the low number of 380 days-old APPtg mice. In addition, at the age of 50 days, whole brain $K_{p,brain}$ values were significantly higher in the APPtg group than in the wild-type group. Moreover, whole brain $K_{p,brain}$ values were significantly higher in tariquidar pre-treated Abcb1a/b$^{(+/-)}$ mice (with a 50% reduction in P-gp expression) than in tariquidar pre-treated wild-type mice. In Figure 2(c), the percentage increase in whole brain $K_{p,brain}$ values in tariquidar pre-treated versus vehicle pre-treated animals is summarized, indicating significantly higher increases in Abcb1a/b$^{(+/-)}$ mice than in 50 days-old wild-type mice. In both, the wild-type and the APPtg group, there was a trend for higher increases in whole brain $K_{p,brain}$ values with increasing age (Figure 2(c)).

We outlined hippocampus and cortex as brain regions with substantial Aβ deposition and cerebellum as a control region with minimal Aβ deposition in all tariquidar pre-treated groups (Supplementary Figures 3 and 4). Regional $K_{p,brain}$ values in different tariquidar pre-treated groups are summarized in Figure 3. Similar differences in $K_{p,brain}$ values as for the whole brain region (Figure 2) were found between different groups

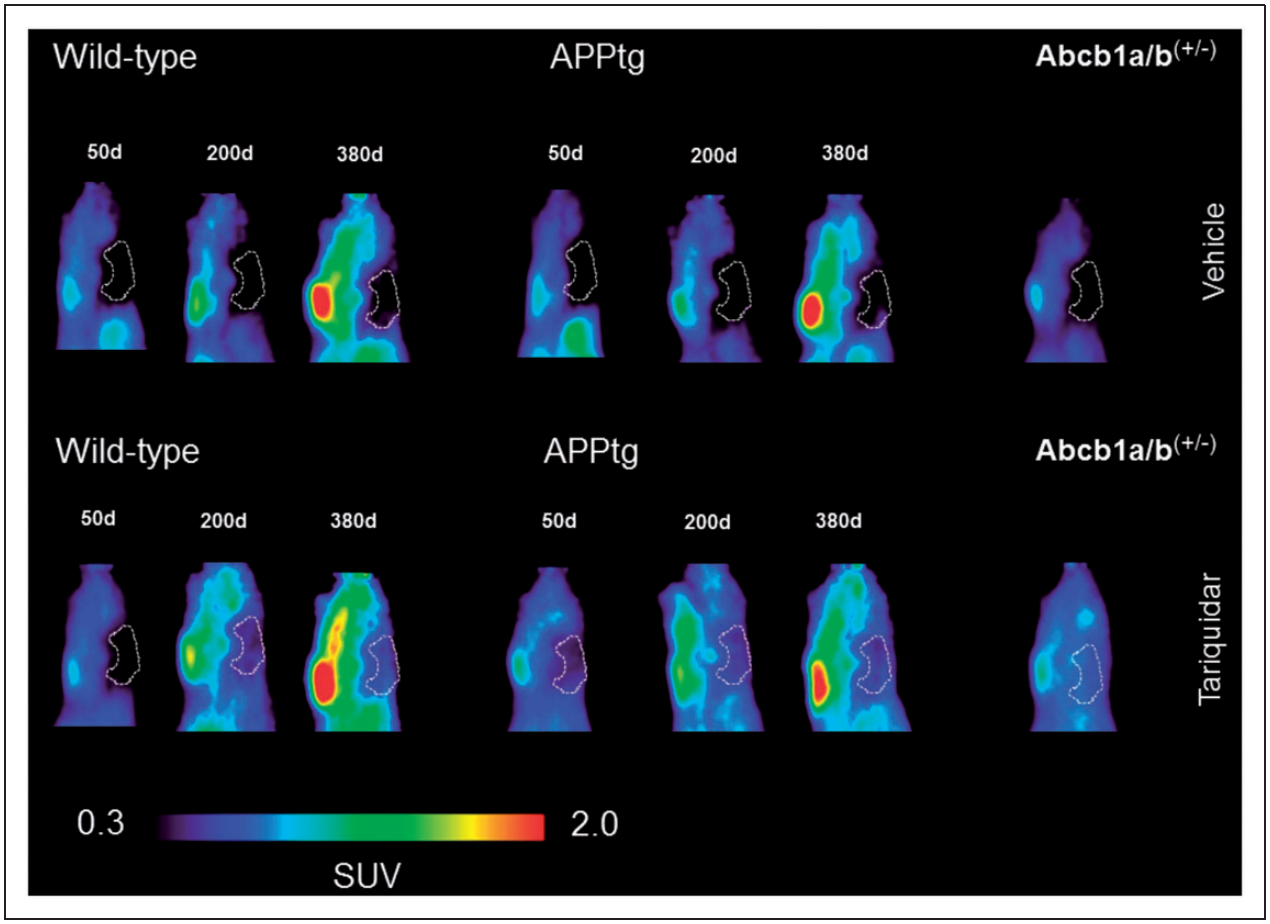

Figure 1. Sagittal PET summation images (0–60 min) of wild-type and APPtg mice aged 50, 200 and 380 days and Abcb1a/b$^{(+/-)}$ mice pre-treated i.v. with vehicle or tariquidar (4 mg/kg) at 2 h before start of the PET scan. Whole brain region is highlighted as a white broken line. All images are set to the same intensity scale (0.3–2.0 standardized uptake value, SUV).

in the hippocampus (Figure 3(a)) and the cortex (Figure 3(b)). On the other hand, in the cerebellum, significant differences in $K_{p,brain}$ values were only found between 50 and 380 days-old wild-type mice (Figure 3(c)).

To exclude that the observed differences in $K_{p,brain}$ values between the different groups were due to differences in radiotracer metabolism, we used radio-TLC to determine the percentage of unchanged (*R*)-[^{11}C]verapamil in the plasma samples collected at the end of the PET scan. In both, vehicle and tariquidar pre-treated animals, the percentage of unchanged (*R*)-[^{11}C]verapamil was not significantly different between wild-type and APPtg mice aged 50 and 200 days, respectively. In tariquidar pre-treated wild-type mice aged 50 and 200 days $26.0 \pm 2.7\%$ and $26.7 \pm 9.9\%$ of total plasma radioactivity was in the form of unchanged (*R*)-[^{11}C]verapamil, while these values were $23.4 \pm 6.5\%$ and $30.5 \pm 8.2\%$ in 50 and 200 days-old APPtg mice, respectively.

P-gp was immunohistochemically stained in brain slices of wild-type and APPtg mice (Figure 4). A semi-quantitative analysis of the stained microvessels indicated significantly decreased P-gp levels in the hippocampus of APPtg versus wild-type mice of all three age groups (Figure 5(a)). Moreover, there was a significant age-dependent decrease in P-gp levels in the hippocampus of both wild-type and APPtg mice. In the cortex, the differences in P-gp levels seen in the hippocampus were less pronounced (Figure 5(b)), while they were almost absent in the cerebellum except for a significant difference in P-gp between 50 and 200 days-old wild-type mice (Figure 5(c)). P-gp levels in the cerebellum were lower than in the other two brain regions. Immunohistochemical analysis confirmed that Abcb1a/b$^{(+/-)}$ mice had approximately 50% less P-gp in the hippocampus and cortex than wild-type mice. In tariquidar pre-treated animal groups, there was a significant negative correlation between $K_{p,brain}$ values and P-gp levels in the hippocampus, a trend for a negative

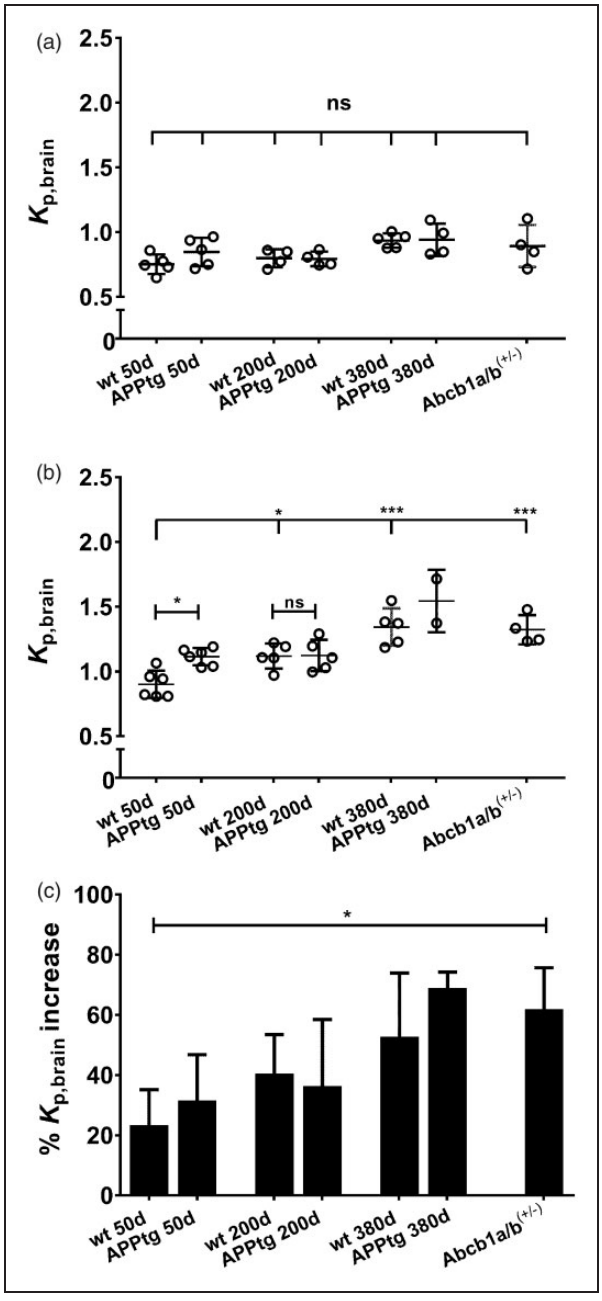

Figure 2. Whole brain-to-plasma radioactivity concentration ratios at the end of the PET scan ($K_{p,brain}$) in wild-type and APPtg mice aged 50, 200 and 380 days and in Abcb1a/b$^{(+/-)}$ mice pre-treated i.v. with vehicle (a) or with tariquidar (4 mg/kg) at 2 h before start of the PET scan (b). Lines indicate mean ± standard deviation. In (c) the mean (+ standard deviation) percentage increase in $K_{p,brain}$ of individual tariquidar treated animals relative to mean $K_{p,brain}$ value of vehicle group is shown. Ns: not significant, *$P < 0.05$, ***$P < 0.001$, 1-way ANOVA followed by Tukey's multiple comparison test.

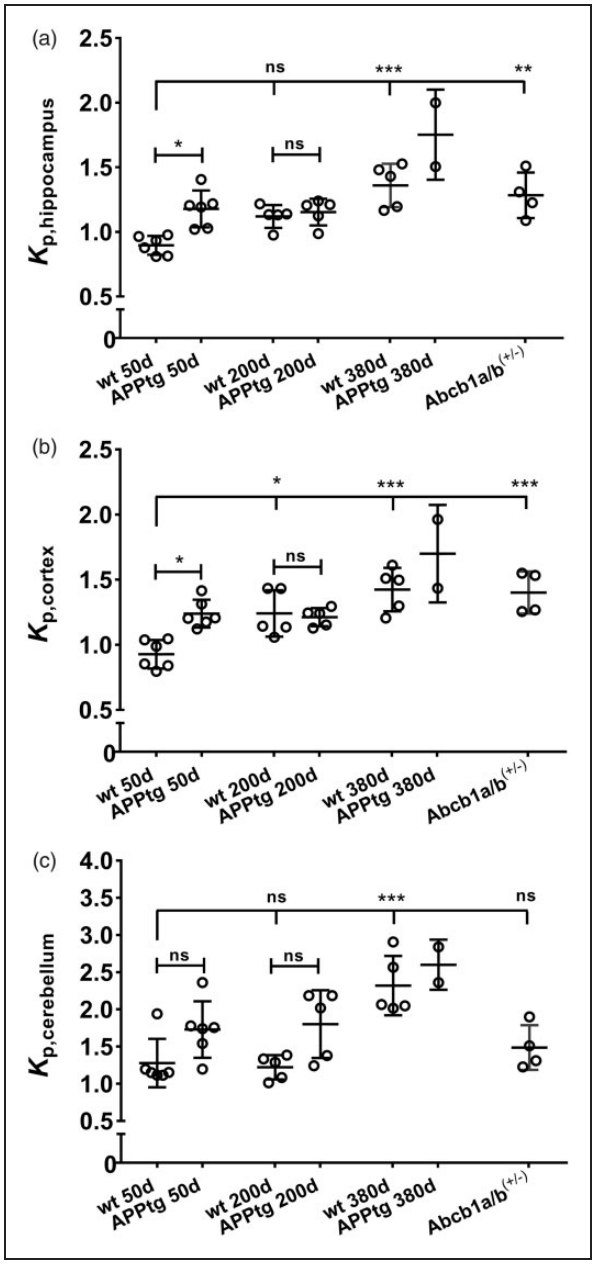

Figure 3. Regional brain-to-plasma radioactivity concentration ratios at the end of the PET scan ($K_{p,brain}$) for hippocampus (a), cortex (b) and cerebellum (c) in wild-type and APPtg mice aged 50, 200 and 380 days and in Abcb1a/b$^{(+/-)}$ mice pre-treated i.v. with tariquidar (4 mg/kg) at 2 h before start of the PET scan. Lines indicate mean ± standard deviation. Ns: not significant, *$P < 0.05$, **$P < 0.01$, ***$P < 0.001$, one-way ANOVA followed by Tukey's multiple comparison test.

correlation in the cortex and no correlation in the cerebellum (Supplementary Figure 5).

In addition, we immunohistochemically analyzed Aβ load in all animal groups and found substantial Aβ deposition in the hippocampus and cortex of APPtg mice aged 200 and 380 days and almost no Aβ deposition in the cerebellum (Figure 6). In the hippocampus and cortex of APPtg mice, Aβ deposition significantly increased with age. In wild-type mice, no Aβ deposition could be detected in all investigated brain regions.

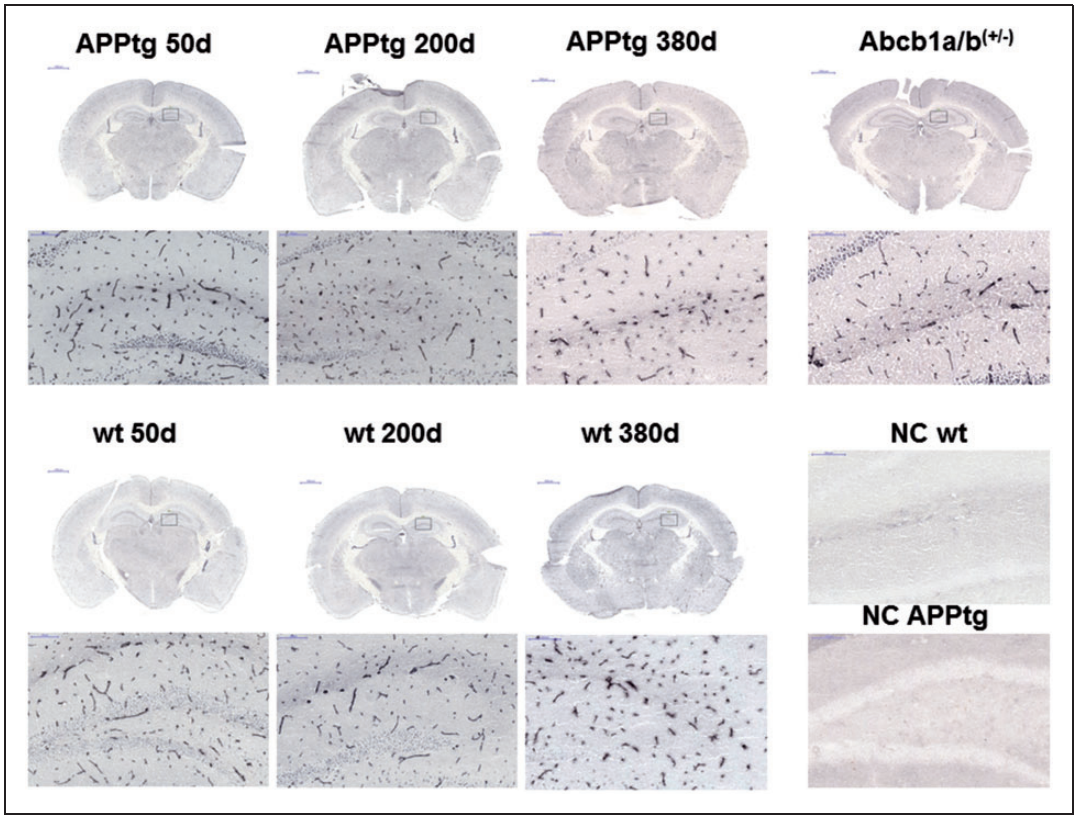

Figure 4. Immunohistochemical staining of P-gp in brain microvessels of wild-type and APPtg mice aged 50, 200 and 380 days and in Abcb1a/b$^{(+/-)}$ mice. An enlarged section of the area corresponding to the hippocampus region (black square) is shown at a 20 × magnification below each image. Negative controls (NC) of the hippocampus region in a wild-type and an APPtg mouse are depicted at 20 × magnification.

Discussion

In the present study, we used (*R*)-[^{11}C]verapamil PET in combination with tariquidar to assess the age dependency of cerebral P-gp function in a frequently employed AD mouse model (APPtg mice)[35] and in wild-type control mice. The employed model rapidly develops extensive cerebral Aβ deposits from an age of three months onwards. Accordingly, immunohistochemical analysis confirmed a substantial amount of Aβ deposits in the hippocampus and cortex of APPtg mice aged 200 and 380 days (Figure 6). Surprisingly, despite the widespread use of transgenic mouse models in AD research, no attempts have been made so far to measure cerebral P-gp function with PET in AD mouse models. Brain distribution of diverse P-gp substrates has been assessed in AD mouse models,[11,36,37] which failed to confirm alterations relative to age-matched control mice, despite a reduction in cerebral P-gp expression.[11] Gustafsson et al.[37] found no significant differences in the ratio of unbound brain to unbound plasma concentration ($K_{p,uu,brain}$) of the P-gp substrates digoxin and paliperidone between tg-APP_{ArcSwe} and age-matched control mice. Similarly, Mehta et al.[11] found an unchanged brain distribution of digoxin, verapamil and loperamide in triple transgenic AD mice harboring three mutant genes (APP_{swe}, PS-1_{M146V} and tau_{P301L}). This was attributed by Mehta et al.[11] to a thickening of the basement membrane of the BBB in AD mice, which may have impeded transcellular diffusion and thereby counteracted the reduction in P-gp expression. An alternative explanation for the failure of Mehta et al.[11] to detect increases in brain distribution of verapamil and loperamide in their AD mouse model may be related to the capacity of P-gp to functionally compensate moderate reductions in its expression. This phenomenon is similar to the well-described functional interplay between P-gp and breast cancer resistance protein (BCRP, ABCG2) at the mouse and human BBB in limiting brain distribution of dual P-gp/BCRP substrates.[38,39] When only one transporter is knocked out or inhibited, the other transporter effectively limits brain distribution of dual substrates. We have shown that brain distribution of (*R*)-[^{11}C]verapamil and [^{11}C]*N*-desmethyl-loperamide is increased only by 1.5- and 1.1-fold, respectively, in heterozygous P-gp knockout mice (Abcb1a/b$^{(+/-)}$), which have a 50%

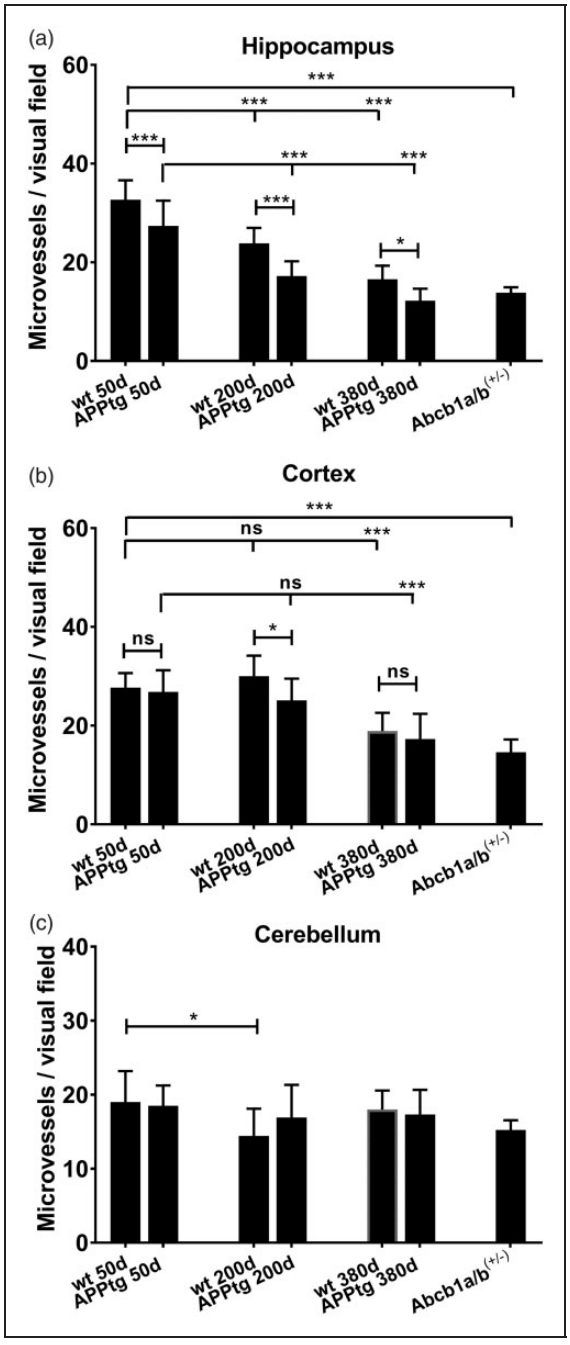

Figure 5. Semi-quantitative evaluation of stained microvessels in the hippocampus (a), the cortex (b) and the cerebellum (c) of 50, 200 and 380 days-old wild-type and APPtg mice and of Abcb1a/b$^{(+/-)}$ mice. Four visual fields (20 × magnification) per mouse ($n = 3$–5 animals per group) were counted and the mean of each group was calculated. Error bars indicate standard deviation. Ns: not significant, *$P < 0.05$, ***$P < 0.001$, one-way ANOVA followed by Tukey's multiple comparison test.

reduction in P-gp expression at the BBB, as compared with wild-type mice.[28] In contrast, in homozygous P-gp knockout mice (Abcb1a/b$^{(-/-)}$), which completely lack P-gp, brain distribution of (*R*)-[^{11}C]verapamil and [^{11}C]*N*-desmethyl-loperamide was enhanced by 3.9- and 2.8-fold, respectively, relative to wild-type mice. In accordance with these data, PET studies with (*R*)-[^{11}C]verapamil or [^{11}C]verapamil in AD patients revealed only moderate changes in radiotracer brain distribution as compared with age-matched control subjects.[40,41] Van Assema et al.[40] found no differences between AD subjects and control subjects in total volume of distribution (V_T) and influx rate constant of (*R*)-[^{11}C]verapamil from plasma into brain (K_1),[40] two parameters which have been associated with P-gp function at the BBB.[23,42] However, these authors reported a significant increase in the non-displaceable binding potential (BP_{ND}) of (*R*)-[^{11}C]verapamil, which they hypothesized to reflect decreased P-gp function. A study by Deo et al.[41] could only reveal regional differences in [^{11}C]verapamil brain distribution between AD and control subjects, when regional K_1 values were normalized to cerebral blood flow, which was lower in AD patients. Other than these two PET studies in AD patients, a few studies have assessed differences in cerebral P-gp function between elderly and young healthy volunteers with [^{11}C]verapamil or (*R*)-[^{11}C]verapamil PET.[43–46] These studies found moderate increases (15–20%) in radiotracer brain distribution in elderly subjects,[43–45] pointing to an age-dependent decrease in P-gp function. In a recent study, we examined young and elderly healthy volunteers with (*R*)-[^{11}C]verapamil PET and found no differences in whole brain V_T values in baseline scans, while significant differences were found in PET scans performed after administration of tariquidar at a dose of 3 mg/kg, leading to partial P-gp inhibition at the human BBB.[32] These data supported the concept that the partial P-gp inhibition PET protocol possesses a higher sensitivity to detect an age-related reduction in cerebral P-gp expression than (*R*)-[^{11}C]verapamil baseline scans without inhibitor administration. These results prompted us to employ the partial P-gp inhibition protocol in the present preclinical PET study.

As an outcome parameter of (*R*)-[^{11}C]verapamil brain distribution, we used $K_{p,brain}$, which we have shown in a previous study to display an excellent correlation with V_T derived from kinetic modeling.[28] The advantage of $K_{p,brain}$ is that it does not require repeated arterial blood sampling, which is technically difficult in mice. In addition, we have shown that $K_{p,brain}$ of (*R*)-[^{11}C]verapamil is independent of cerebral blood flow in mice.[28] In line with our human data [32] and the data by Mehta et al.,[11] no differences in (*R*)-[^{11}C]verapamil $K_{p,brain}$ values were found between APPtg and control mice in baseline scans without tariquidar administration (Figure 2(a)). However, after partial P-gp inhibition, significant differences in (*R*)-[^{11}C]verapamil $K_{p,brain}$ values became apparent

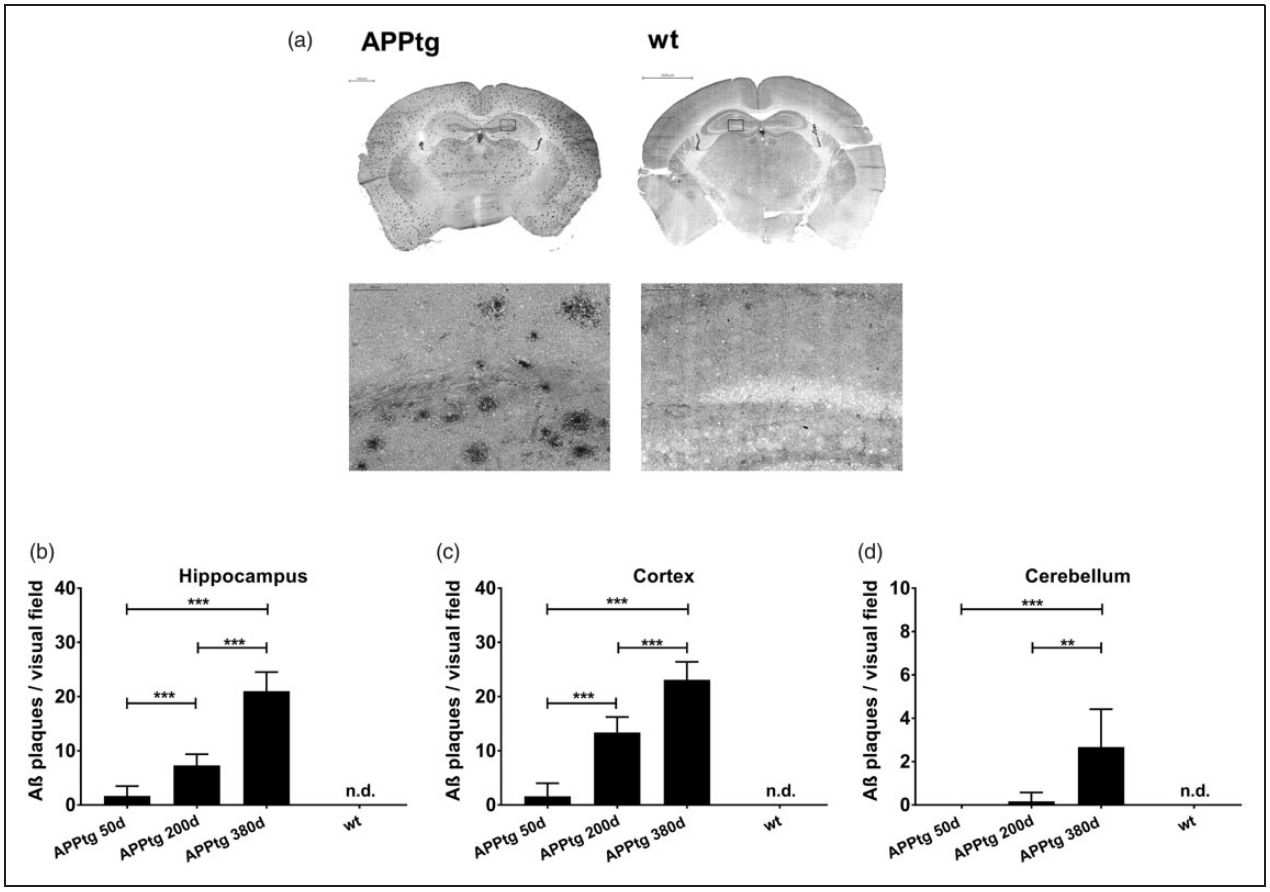

Figure 6. Immunohistochemical staining of Aβ in brains of wild-type and APPtg mice aged 380 days. An enlarged section of the area corresponding to the hippocampus region (black square) is shown at a 20 × magnification below each image (a). Semi-quantitative evaluation of stained Aβ in the hippocampus (b), the cortex (c) and the cerebellum (d) of 50, 200 and 380 days-old APPtg mice and 380 days-old wild-type mice. Four visual fields (20 × magnification) per mouse ($n = 3$–5 animals per group) were counted and the mean of each group was calculated (n.d.: not detected). Error bars indicate standard deviation. Ns: not significant, $^{*}P < 0.05$, $^{**}P < 0.01$, one-way ANOVA followed by Tukey's multiple comparison test.

(Figure 2(b)). To support the validity of our imaging protocol, we also examined Abcb1a/b$^{(+/-)}$ mice, which have a 50% reduction in cerebral P-gp expression (Figure 5). In agreement with their decreased P-gp expression, $K_{p,brain}$ values were significantly higher in Abcb1a/b$^{(+/-)}$ mice after partial P-gp inhibition as compared with wild-type mice (Figure 2(b)). In the hippocampus, $K_{p,brain}$ values after tariquidar pre-treatment showed a significant negative correlation with P-gp levels determined with immunohistochemistry, which supported that our PET protocol effectively measured P-gp function in the brain (Supplementary Figure 5). Intriguingly, (*R*)-[^{11}C]verapamil $K_{p,brain}$ values were significantly higher in APPtg mice than in control mice at a young age of 50 days. At this age, mostly monomeric Aβ and soluble oligomers are present in the brain of this mouse model, while plaques are scarcely present and cognitive impairment is not detectable for at least another month.[35,47] These findings agree well with data by Hartz et al.[8] who found in another AD mouse model (Tg2576 mice) a significant decrease in P-gp levels and transport capacity at an age of 12 weeks, at which no cognitive symptoms were present. Interestingly, no significant differences in (*R*)-[^{11}C]verapamil $K_{p,brain}$ values could be found in our study between APPtg and wild-type mice at the age of 200 days. A possible explanation for this could be that differences in P-gp function between APPtg and wild-type mice were masked with increasing age by additional alterations in the BBB (e.g. thickening of the basement membrane) or a reduction in cerebral blood flow in APPtg mice.

We found both in APPtg and control mice an age-dependent increase in $K_{p,brain}$ values. At the age of 380 days, $K_{p,brain}$ values reached both in APPtg and control mice similar levels as in Abcb1a/b$^{(+/-)}$ mice, which suggested that the age-related reduction in P-gp function was of the order of −50% (Figure 2(b)). Our data are in good agreement with other studies, which showed that

expression of P-gp protein and mRNA levels declined over age in healthy rats.[48–50] However, with one exception,[50] none of these studies investigated the functional consequences of this age-related decline in P-gp expression. A study by Bors et al.[50] measured brain concentrations of the P-gp substrate quinidine with cerebral microdialysis in middle-aged (12–14 months) and young rats (2–3 months) and found 22% higher brain-to-blood AUC ratios and delayed elimination of quinidine from the brain in middle aged rats. Our study confirms previous findings of an inverse relationship between cerebral Aβ load and P-gp function,[51] in that the observed age- and disease-related increases in (*R*)-[^{11}C]verapamil $K_{p,brain}$ values were more pronounced in brain regions with extensive Aβ deposition (hippocampus, cortex) than in a region with negligible Aβ deposition (cerebellum) (Figure 3). The exact mechanism by which Aβ deposition leads to a reduction in P-gp levels has not been elucidated yet. Hartz et al.[52] proposed that Aβ40 leads to ubiquitination, internalization and proteosomal degradation of P-gp. Our observation that P-gp function was already decreased at a young age of 50 days, at which no Aβ deposits were visible, is in accordance with the results by Hartz et al., who showed that degradation of P-gp is triggered by soluble Aβ forms. Our data support the concept that early treatment of AD patients with P-gp inducing drugs may be an interesting strategy to restore P-gp function at the BBB thereby delaying the build-up of Aβ deposits in the brain.[4,8,16]

We have shown in this study that our partial P-gp-inhibition (*R*)-[^{11}C]verapamil PET protocol possesses adequate sensitivity to measure reduced P-gp function in an AD mouse model. This PET protocol can readily and safely be applied in human subjects[31,32] and may therefore be of interest to monitor the efficacy of P-gp inducing drugs in humans. The only study, which has so far attempted to measure P-gp induction at the human BBB with PET, failed to detect changes in [^{11}C]verapamil brain distribution after treatment of healthy volunteers with the pregnane X receptor (PXR) ligand rifampicin, which may be related to the limited sensitivity of [^{11}C]verapamil baseline scans to detect moderate changes in cerebral P-gp function.[53] Following the concept of precision medicine, our PET protocol may help selecting AD patients, in whom cerebral P-gp function is impaired, for a treatment with P-gp inducing drugs. A disadvantage of our PET protocol is that it requires i.v. administration of tariquidar, which is a non-marketed drug with limited availability for clinical use. In addition, the use of tariquidar may lead to drug–drug interactions with concomitant medication used in patients, which needs to be considered when employing this PET protocol. However, as our PET protocol requires only one single administration of tariquidar at a dose, which only partially inhibits P-gp at the BBB, the safety concerns associated with the use of tariquidar in patients may be manageable. Indeed, our PET protocol has already been safely used in drug resistant temporal lobe epilepsy patients.[31] Another possible limitation of our PET protocol is related to the fact that (*R*)-[^{11}C]verapamil undergoes CYP3A4-mediated metabolism giving radiolabeled metabolites, which are taken up into the brain.[28,54] P-gp inducing drugs may alter (*R*)-[^{11}C]verapamil metabolism, thereby masking their P-gp inducing effects. However, our previous data have shown that metabolism of (*R*)-[^{11}C]verapamil is considerably slower in humans than in rodents.[25,42] Moreover, the consideration of early PET data in the data analysis may overcome the potential bias of brain uptake of radiolabeled metabolites.[23,31] In the present PET study, we showed that the percentage of unchanged (*R*)-[^{11}C]verapamil in plasma was similar in the investigated groups, which ruled out that the observed differences in $K_{p,brain}$ values were due to differences in radiotracer metabolism.

The observed age-related decline in P-gp function at the BBB may not only have an effect on Aβ clearance but may also lead to increased brain distribution of P-gp substrate drugs and an increased risk of P-gp mediated drug–drug interactions at the BBB.[32] This is of clinical relevance as AD patients often take several different drugs on a regular basis. Concomitant intake of two drugs, which are both transported by P-gp at the BBB, may lead to partial saturation of P-gp and may increase brain distribution of one of these drugs. These changes may be greater in AD patients as compared with healthy people potentially leading to an increased incidence of adverse events.

Conclusion

We demonstrated that (*R*)-[^{11}C]verapamil PET in combination with tariquidar possesses an adequate sensitivity to measure changes in cerebral P-gp function in APPtg mice versus wild-type control mice. Our results confirm previous findings that P-gp function is reduced in AD mouse models. Moreover, we were able to demonstrate a significant, up to 50% age-related decline in cerebral P-gp function in wild-type and APPtg mice. Importantly, we found significant differences in cerebral P-gp function between wild-type and APPtg mice at a young age of 50 days, which suggests that impaired P-gp function is present before substantial deposition of Aβ and cognitive decline occurs. This underlines that pharmacological strategies to enhance P-gp function at the BBB may be a useful approach to increase Aβ clearance across the BBB thereby potentially delaying the onset and slowing the progression of AD. Our PET

protocol may be employed in future studies to test the efficacy of different P-gp induction protocols in humans.

Funding

The author(s) disclosed receipt of the following financial support for the research, authorship, and/or publication of this article: This work was supported by the Austrian Science Fund (FWF) [grant number I 1609-B24, to O. Langer], the Deutsche Forschungsgemeinschaft (DFG) [grant number DFG PA930/9-1, to J. Pahnke] and the Lower Austria Corporation for Research and Education (NFB) [grant number LS14-008, to T. Wanek].

Acknowledgements

The authors wish to thank Mathilde Löbsch for help in conducting the PET experiments and Helena Schuller (University of Applied Sciences, Wiener Neustadt, Austria) for Aβ immunohistochemistry.

Declaration of conflicting interests

The author(s) declared no potential conflicts of interest with respect to the research, authorship, and/or publication of this article.

Authors' contributions

Oliver Langer, Thomas Wanek, Thomas Pekar, Martin Bauer and Jens Pahnke designed the research; Viktoria Zoufal, Markus Krohn, Severin Mairinger, Thomas Filip, Michael Sauberer and Johann Stanek performed the research; Viktoria Zoufal and Thomas Wanek analyzed the data; Oliver Langer, Viktoria Zoufal and Thomas Wanek wrote the paper.

Supplementary material

Supplementary material for this paper can be found at the journal website: http://journals.sagepub.com/home/jcb

References

1. Tiraboschi P, Hansen LA, Thal LJ, et al. The importance of neuritic plaques and tangles to the development and evolution of AD. *Neurology* 2004; 62: 1984–1989.
2. Hardy J and Allsop D. Amyloid deposition as the central event in the aetiology of Alzheimer's disease. *Trends Pharmacol Sci* 1991; 12: 383–388.
3. Vogelgesang S, Warzok RW, Cascorbi I, et al. The role of P-glycoprotein in cerebral amyloid angiopathy; implications for the early pathogenesis of Alzheimer's disease. *Curr Alzheimer Res* 2004; 1: 121–125.
4. Pahnke J, Walker LC, Scheffler K, et al. Alzheimer's disease and blood-brain barrier function-Why have anti-beta-amyloid therapies failed to prevent dementia progression? *Neurosci Biobehav Rev* 2009; 33: 1099–1108.
5. Shibata M, Yamada S, Kumar SR, et al. Clearance of Alzheimer's amyloid-ss(1-40) peptide from brain by LDL receptor-related protein-1 at the blood-brain barrier. *J Clin Invest* 2000; 106: 1489–1499.
6. Storck SE, Meister S, Nahrath J, et al. Endothelial LRP1 transports amyloid-beta(1-42) across the blood-brain barrier. *J Clin Invest* 2016; 126: 123–136.
7. Lam FC, Liu R, Lu P, et al. beta-Amyloid efflux mediated by p-glycoprotein. *J Neurochem* 2001; 76: 1121–1128.
8. Hartz AM, Miller DS and Bauer B. Restoring blood-brain barrier P-glycoprotein reduces brain amyloid-beta in a mouse model of Alzheimer's disease. *Mol Pharmacol* 2010; 77: 715–723.
9. Cirrito JR, Deane R, Fagan AM, et al. P-glycoprotein deficiency at the blood-brain barrier increases amyloid-beta deposition in an Alzheimer disease mouse model. *J Clin Invest* 2005; 115: 3285–3290.
10. Kuhnke D, Jedlitschky G, Grube M, et al. MDR1-P-glycoprotein (ABCB1) mediates transport of Alzheimer's amyloid-beta peptides – implications for the mechanisms of Abeta clearance at the blood-brain barrier. *Brain Pathol* 2007; 17: 347–353.
11. Mehta DC, Short JL and Nicolazzo JA. Altered brain uptake of therapeutics in a triple transgenic mouse model of Alzheimer's disease. *Pharm Res* 2013; 30: 2868–2879.
12. Wijesuriya HC, Bullock JY, Faull RL, et al. ABC efflux transporters in brain vasculature of Alzheimer's subjects. *Brain Res* 2010; 1358: 228–238.
13. Kannan P, Schain M, Kretzschmar WW, et al. An automated method measures variability in P-glycoprotein and ABCG2 densities across brain regions and brain matter. *J Cereb Blood Flow Metab* 2017; 37: 2062–2075.
14. Jeynes B and Provias J. An investigation into the role of P-glycoprotein in Alzheimer's disease lesion pathogenesis. *Neurosci Lett* 2011; 487: 389–393.
15. Carrano A, Snkhchyan H, Kooij G, et al. ATP-binding cassette transporters P-glycoprotein and breast cancer related protein are reduced in capillary cerebral amyloid angiopathy. *Neurobiol Aging* 2014; 35: 565–575.
16. Pahnke J, Frohlich C, Paarmann K, et al. Cerebral ABC transporter-common mechanisms may modulate neurodegenerative diseases and depression in elderly subjects. *Arch Med Res* 2014; 45: 738–743.
17. Abuznait AH, Qosa H, Busnena BA, et al. Olive-oil-derived oleocanthal enhances beta-amyloid clearance as a potential neuroprotective mechanism against Alzheimer's disease: in vitro and in vivo studies. *ACS Chem Neurosci* 2013; 4: 973–82.
18. Brenn A, Grube M, Jedlitschky G, et al. St. John's Wort reduces beta-amyloid accumulation in a double transgenic Alzheimer's disease mouse model-role of P-glycoprotein. *Brain Pathol* 2014; 24: 18–24.
19. Durk MR, Han K, Chow EC, et al. 1alpha,25-Dihydroxyvitamin D3 reduces cerebral amyloid-beta accumulation and improves cognition in mouse models of Alzheimer's disease. *J Neurosci* 2014; 34: 7091–7101.
20. Mohamed LA, Keller JN and Kaddoumi A. Role of P-glycoprotein in mediating rivastigmine effect on amyloid-beta brain load and related pathology in Alzheimer's disease mouse model. *Biochim Biophys Acta* 2016; 1862: 778–787.

21. Wanek T, Mairinger S and Langer O. Radioligands targeting P-glycoprotein and other drug efflux proteins at the blood–brain barrier. *J Labelled Comp Radiopharm* 2013; 56: 68–77.
22. Raaphorst RM, Windhorst AD, Elsinga PH, et al. Radiopharmaceuticals for assessing ABC transporters at the blood-brain barrier. *Clin Pharmacol Ther* 2015; 97: 362–371.
23. Muzi M, Mankoff DA, Link JM, et al. Imaging of cyclosporine inhibition of P-glycoprotein activity using ^{11}C-verapamil in the brain: studies of healthy humans. *J Nucl Med* 2009; 50: 1267–1275.
24. Liow JS, Kreisl W, Zoghbi SS, et al. P-glycoprotein function at the blood-brain barrier imaged using ^{11}C-N-desmethyl-loperamide in monkeys. *J Nucl Med* 2009; 50: 108–115.
25. Kuntner C, Bankstahl JP, Bankstahl M, et al. Dose-response assessment of tariquidar and elacridar and regional quantification of P-glycoprotein inhibition at the rat blood-brain barrier using (*R*)-[^{11}C]verapamil PET. *Eur J Nucl Med Mol Imaging* 2010; 37: 942–953.
26. Kreisl WC, Bhatia R, Morse CL, et al. Increased permeability-glycoprotein inhibition at the human blood-brain barrier can be safely achieved by performing PET during peak plasma concentrations of tariquidar. *J Nucl Med* 2015; 56: 82–87.
27. Bauer M, Karch R, Zeitlinger M, et al. Approaching complete inhibition of P-glycoprotein at the human blood-brain barrier: an (*R*)-[^{11}C]verapamil PET study. *J Cereb Blood Flow Metab* 2015; 35: 743–746.
28. Wanek T, Römermann K, Mairinger S, et al. Factors governing p-glycoprotein-mediated drug-drug interactions at the blood-brain barrier measured with positron emission tomography. *Mol Pharm* 2015; 12: 3214–3225.
29. Kannan P, John C, Zoghbi SS, et al. Imaging the function of P-glycoprotein with radiotracers: pharmacokinetics and in vivo applications. *Clin Pharmacol Ther* 2009; 86: 368–377.
30. Bankstahl JP, Bankstahl M, Kuntner C, et al. A novel PET imaging protocol identifies seizure-induced regional overactivity of P-glycoprotein at the blood-brain barrier. *J Neurosci* 2011; 31: 8803–8811.
31. Feldmann M, Asselin M-C, Liu J, et al. P-glycoprotein expression and function in patients with temporal lobe epilepsy: a case-control study. *Lancet Neurol* 2013; 12: 777–785.
32. Bauer M, Wulkersdorfer B, Karch R, et al. Effect of P-glycoprotein inhibition at the blood-brain barrier on brain distribution of (*R*)-[^{11}C]verapamil in elderly vs. young subjects. *Br J Clin Pharmacol* 2017; 83: 1991–1999.
33. la Fougère C, Boning G, Bartmann H, et al. Uptake and binding of the serotonin 5-HT$_{1A}$ antagonist [^{18}F]-MPPF in brain of rats: effects of the novel P-glycoprotein inhibitor tariquidar. *Neuroimage* 2010; 49: 1406–1415.
34. Bartmann H, Fuest C, la Fougère C, et al. Imaging of P-glycoprotein-mediated pharmacoresistance in the hippocampus: proof-of-concept in a chronic rat model of temporal lobe epilepsy. *Epilepsia* 2010; 51: 1780–1790.
35. Radde R, Bolmont T, Kaeser SA, et al. Abeta42-driven cerebral amyloidosis in transgenic mice reveals early and robust pathology. *EMBO Rep* 2006; 7: 940–946.
36. Cheng Z, Zhang J, Liu H, et al. Central nervous system penetration for small molecule therapeutic agents does not increase in multiple sclerosis- and Alzheimer's disease-related animal models despite reported blood-brain barrier disruption. *Drug Metab Dispos* 2010; 38: 1355–1361.
37. Gustafsson S, Lindström V, Ingelsson M, et al. Intact blood-brain barrier transport of small molecular drugs in animal models of amyloid beta and alpha-synuclein pathology. *Neuropharmacology* 2018; 128: 482–491.
38. Kodaira H, Kusuhara H, Ushiki J, et al. Kinetic analysis of the cooperation of P-glycoprotein (P-gp/Abcb1) and breast cancer resistance protein (Bcrp/Abcg2) in limiting the brain and testis penetration of erlotinib, flavopiridol, and mitoxantrone. *J Pharmacol Exp Ther* 2010; 333: 788–796.
39. Bauer M, Römermann K, Karch R, et al. Pilot PET study to assess the functional interplay between ABCB1 and ABCG2 at the human blood-brain barrier. *Clin Pharmacol Ther* 2016; 100: 131–141.
40. van Assema DM, Lubberink M, Bauer M, et al. Blood-brain barrier P-glycoprotein function in Alzheimer's disease. *Brain* 2012; 135(Pt 1): 181–189.
41. Deo AK, Borson S, Link JM, et al. Activity of P-glycoprotein, a beta-amyloid transporter at the blood-brain barrier, is compromised in patients with mild Alzheimer disease. *J Nucl Med* 2014; 55: 1106–1111.
42. Wagner CC, Bauer M, Karch R, et al. A pilot study to assess the efficacy of tariquidar to inhibit P-glycoprotein at the human blood-brain barrier with (*R*)-^{11}C-verapamil and PET. *J Nucl Med* 2009; 50: 1954–1961.
43. van Assema DM, Lubberink M, Boellaard R, et al. P-glycoprotein function at the blood-brain barrier: effects of age and gender. *Mol Imaging Biol* 2012; 14: 771–776.
44. Toornvliet R, van Berckel BN, Luurtsema G, et al. Effect of age on functional P-glycoprotein in the blood-brain barrier measured by use of (*R*)-[^{11}C]verapamil and positron emission tomography. *Clin Pharmacol Ther* 2006; 79: 540–548.
45. Bauer M, Karch R, Neumann F, et al. Age dependency of cerebral P-gp function measured with (*R*)-[^{11}C]verapamil and PET. *Eur J Clin Pharmacol* 2009; 65: 941–946.
46. Bartels AL, Kortekaas R, Bart J, et al. Blood-brain barrier P-glycoprotein function decreases in specific brain regions with aging: a possible role in progressive neurodegeneration. *Neurobiol Aging* 2009; 30: 1818–1824.
47. Hofrichter J, Krohn M, Schumacher T, et al. Reduced Alzheimer's disease pathology by St. John's Wort treatment is independent of hyperforin and facilitated by ABCC1 and microglia activation in mice. *Curr Alzheimer Res* 2013; 10: 1057–1069.
48. Silverberg GD, Messier AA, Miller MC, et al. Amyloid efflux transporter expression at the blood-brain barrier declines in normal aging. *J Neuropathol Exp Neurol* 2010; 69: 1034–1043.
49. Osgood D, Miller MC, Messier AA, et al. Aging alters mRNA expression of amyloid transporter genes

at the blood-brain barrier. *Neurobiol Aging* 2017; 57: 178–185.
50. Bors L, Toth K, Toth EZ, et al. Age-dependent changes at the blood-brain barrier. A Comparative structural and functional study in young adult and middle aged rats. *Brain Res Bull* 2018; 139: 269–277.
51. Vogelgesang S, Cascorbi I, Schroeder E, et al. Deposition of Alzheimer's beta-amyloid is inversely correlated with P-glycoprotein expression in the brains of elderly non-demented humans. *Pharmacogenetics* 2002; 12: 535–541.
52. Hartz AM, Zhong Y, Wolf A, et al. Abeta40 reduces P-glycoprotein at the blood-brain barrier through the ubiquitin-proteasome pathway. *J Neurosci* 2016; 36: 1930–1941.
53. Liu L, Collier AC, Link JM, et al. Modulation of P-glycoprotein at the human blood-brain barrier by quinidine or rifampin treatment: a PET imaging study. *Drug Metab Dispos* 2015; 43: 1795–1804.
54. Luurtsema G, Molthoff CF, Schuit RC, et al. Evaluation of (*R*)-[^{11}C]verapamil as PET tracer of P-glycoprotein function in the blood-brain barrier: kinetics and metabolism in the rat. *Nucl Med Biol* 2005; 32: 87–93.